

NCC 1-80

The  $\nu_2$  Bands of  $^{16}\text{O}^{18}\text{O}^{16}\text{O}$  and  $^{16}\text{O}^{16}\text{O}^{18}\text{O}$ : Line Positions and Intensities

LANGLEY  
70-72-CP  
252398  
198

J.-M. Flaud, C. Camy-Peyret, and A. N'Gom  
Laboratoire de Physique Moléculaire et Atmosphérique  
Université Pierre and Marie Curie et CNRS  
Tour 13, 4 Place Jussieu, 75252 Paris Cedex 05, France

V. Malathy Devi  
Department of Physics  
College of William and Mary  
Williamsburg, Virginia 23185

C. P. Rinsland and M. A. H. Smith  
Atmospheric Sciences Division  
NASA Langley Research Center  
Hampton, Virginia 23665-5225

(NASA-TM-101840) THE  $\nu_2$  BANDS OF  
 $\text{O}-^{16}\text{O}-^{18}\text{O}-^{16}\text{O}$  AND  $\text{O}-^{16}\text{O}-^{16}\text{O}-^{18}\text{O}$ : LINE  
POSITIONS AND INTENSITIES (NASA) 19 p

N90-70389

Unclas  
00/72 0252398

19 manuscript pages

3 Tables

3 Figures

Running Title:  $\nu_2$  Bands of  $^{16}\text{O}^{18}\text{O}^{16}\text{O}$  and  $^{16}\text{O}^{16}\text{O}^{18}\text{O}$

Mail Correspondence to:

Dr. J.-M. Flaud

Laboratoire de Physique Moléculaire et Atmosphérique

Université Pierre and Marie Curie et CNRS

Tour 13, 4 Place Jussieu

75252 Paris Cedex 05

FRANCE

### Abstract

Using  $0.005\text{ cm}^{-1}$  resolution room-temperature Fourier transform spectra of  $^{18}\text{O}$ -enriched ozone samples, an extensive analysis of the  $\nu_2$  bands of the two isotopes  $^{16}\text{O}^{18}\text{O}^{16}\text{O}$  and  $^{16}\text{O}^{16}\text{O}^{18}\text{O}$  was performed. Vibration-rotation energy levels of both species deduced from these analyses together with the available microwave data were then reproduced using a Watson A-type Hamiltonian leading to accurate vibrational energies and rotational constants for the ground states (000) and first excited vibrational states (010) of these two isotopic species. The following band centers were obtained:  $\nu_2 (^{16}\text{O}^{18}\text{O}^{16}\text{O}) = 693.3057\text{ cm}^{-1}$ ,  $\nu_2 (^{16}\text{O}^{16}\text{O}^{18}\text{O}) = 684.6134\text{ cm}^{-1}$ . Finally, appropriate expansions of the transformed transition moment operators of the two  $\nu_2$  bands were used to generate a complete list of line positions, intensities, and lower state energies for the two isotopes  $^{16}\text{O}^{18}\text{O}^{16}\text{O}$  and  $^{16}\text{O}^{16}\text{O}^{18}\text{O}$ .

## INTRODUCTION

In a series of previous papers (1-3), we have reported our work concerning the absorption in the 10- $\mu$ m region of the  $\nu_1$  and  $\nu_3$  bands of the isotopic species of ozone  $^{16}O^{18}O^{16}O$ ,  $^{16}O^{16}O^{18}O$ ,  $^{18}O^{16}O^{16}O$ , and  $^{18}O_3$ . This effort was undertaken in order to improve our knowledge of the spectroscopy of the ozone molecule and to generate line parameters (positions, intensities, and lower state energies) useful for atmospheric remote sensing applications (4). Recently, the absorption in the 14- $\mu$ m region by the  $\nu_2$  and  $2\nu_2 - \nu_2$  bands of the main isotopic species  $^{16}O_3$  has been carefully studied (5). To provide an extensive understanding of isotopic ozone absorption in the same spectral region, we present in this paper the results concerning the  $\nu_2$  bands of the two  $^{18}O$ -isotopic ozone variants of primary atmospheric interest,  $^{16}O^{18}O^{16}O$  and  $^{16}O^{16}O^{18}O$ .

## EXPERIMENTAL DETAILS

The spectral data used in the analyses were obtained in June 1985 at room temperature and 0.005-cm<sup>-1</sup> resolution using the Fourier transform spectrometer located in the McMath solar telescope complex at the National Solar Observatory on Kitt Peak. The absorption cell used in these measurements was a 50-cm long 5.08-cm diameter Pyrex tube with Teflon valves. The KCl windows which were cemented onto the ends of the absorption cell were slightly wedged (5-10 mrad) to prevent channeling arising from multiple reflections.

The ozone samples were prepared by carefully mixing known initial pressures of 99.98% pure  $^{16}O_2$  and 95.9% pure  $^{18}O_2$  in the ozone generating system. The samples were generated using the standard silent electric

discharge technique. The discharge was run for ~1 hour during which time liquid ozone was condensed on the wall of a liquid-nitrogen-cooled cold trap. After the discharge was turned off, the excess oxygen was pumped from the ozone generating system. The liquid ozone was then evaporated by allowing the cold trap to warm to room temperature. Recording of the data was started when the pressure had stabilized. Before starting to record the spectra, the absorption cell was conditioned for ozone by generating a sample and keeping it in the cell for a few hours. Additional details concerning the ozone generating method are given in Refs. (1, 4).

Analyses were performed on two spectra recorded with ozone samples generated from oxygen mixtures which contained ~85%  $^{16}\text{O}_2$  and ~15%  $^{18}\text{O}_2$ . The final sample pressures were ~23.2 and ~15.3 Torr in the absorption cell. The sample pressures and temperatures were monitored continuously during the ~1-hour recording time for each spectrum using a 0- to 100-Torr Barocel pressure gauge and a thermocouple kept in contact with the cell wall. The wavenumber scale of each spectrum was established relative to the standards in the  $\nu_2$  band of  $\text{H}_2^{16}\text{O}$  reported by Brown and Toth (6).

#### Line Positions

The pure rotational spectrum in the (010) states of the two isotopic species  $^{16}\text{O}^{16}\text{O}^{18}\text{O}$  and  $^{16}\text{O}^{18}\text{O}^{16}\text{O}$  was previously studied (7) providing a good set of rotational constants for the (010) state of both molecules. Because the rotational constants of the ground states were also known (8), it was possible to generate a calculated list of line positions for the  $\nu_2$  bands of the two isotopic species with only the band centers as unknown quantities. After several attempts, the comparison between the observed and calculated spectra allowed us to determine these band centers and to assign transitions involving low and medium J and  $K_a$  values. These transitions were fitted

with a Watson-type Hamiltonian to obtain the vibration energies and an improved set of rotational constants for the (010) states. These constants were then used to extend the assignments by extrapolation to new lines with higher  $J$  and  $K_a$  values. However, for  $K_a$  values higher than 11, the ground-state levels calculated using the rotational constants derived from microwave transitions (8) were found to diverge from the observed values with discrepancies between observation and calculation increasing with increasing  $K_a$  values. It was, therefore, necessary to improve the ground-state constants, which was accomplished by fitting simultaneously the available microwave data of the (000) state (8) and the combination differences derived from our infrared spectra. The molecular constants resulting from these fits are given in Tables I and II for the  $^{16}\text{O}^{18}\text{O}^{16}\text{O}$  and  $^{16}\text{O}^{16}\text{O}^{18}\text{O}$  molecules, respectively. These constants are similar to those derived from the microwave spectrum (8) but allow a more precise calculation of the high  $K_a$  levels. The (000) levels calculated from these constants were then used to determine the (010) experimental levels which were reproduced with the aid of a Watson-type Hamiltonian. The corresponding vibrational energies and rotational constants are gathered in Tables I and II for the  $^{16}\text{O}^{18}\text{O}^{16}\text{O}$  and  $^{16}\text{O}^{16}\text{O}^{18}\text{O}$  isotopes, respectively.

### Line Intensities

As in our previous studies (1-3) of the spectra of the  $^{18}\text{O}$  isotopic species of ozone, we faced the problem of determining the line intensities of a molecule for which a pure sample cannot be produced. We, therefore, decided to use theory to calculate the line intensities of the  $\nu_2$  band of the symmetrical molecule  $^{16}\text{O}^{18}\text{O}^{16}\text{O}$ . This was done by transferring the dipole moment of  $^{18}\text{O}$ , using the theory developed in Ref. (9), and the expansion of the transition moment operator of the  $\nu_2$  band of  $^{16}\text{O}^{18}\text{O}^{16}\text{O}$  derived in this

manner is given in Table III. Using this expansion together with the wavefunctions deduced from the energy calculation, the line intensities of the  $\nu_2$  band of  $^{16}\text{O}^{18}\text{O}^{16}\text{O}$  were computed and used to calibrate the spectra. Then, assuming a ratio of 2 between the amounts of  $^{16}\text{O}^{16}\text{O}^{18}\text{O}$  and  $^{16}\text{O}^{18}\text{O}^{16}\text{O}$  in the sample, line intensities of 60 transitions for the  $^{16}\text{O}^{18}\text{O}^{16}\text{O}$  molecule were measured and least-squares fitted leading to the expansion of the transformed transition moment of the B-type component of the  $\nu_2$  band of  $^{16}\text{O}^{16}\text{O}^{18}\text{O}$  which is given in Table III. It is well known that  $^{16}\text{O}^{16}\text{O}^{18}\text{O}$  molecule belongs to the  $C_s$  point group and, consequently, each band of this molecule is a hybrid consisting of a B-type and an A-type component. The B-type component was clearly observed. However, because the spectrum was very crowded, it was not possible to observe the A-type component which is much weaker than the B-type one.

Finally, using the wavefunctions derived from the diagonalization of the Hamiltonian matrices both for the ground and the (010) states, as well as the expansions of the transition moment operators quoted in Table III, a listing of line positions and intensities of the  $\nu_2$  band of  $^{16}\text{O}^{18}\text{O}^{16}\text{O}$  and of the B-type component of the  $\nu_2$  band of  $^{16}\text{O}^{16}\text{O}^{18}\text{O}$  was computed. The calculations were performed up to maximum values of  $J$ ,  $K_a$ , and  $E''$ , respectively, of 65, 17, and  $1750\text{ cm}^{-1}$  with an intensity cutoff of  $0.25 \times 10^{-22}$  and  $0.50 \times 10^{-22}\text{ cm}^{-1}/\text{molecule cm}^{-2}$  at 296 K for the  $^{16}\text{O}^{16}\text{O}^{18}\text{O}$  and  $^{16}\text{O}^{18}\text{O}^{16}\text{O}$  molecules, respectively. The resulting total band intensities are  $0.649 \times 10^{-18}$  and  $0.645 \times 10^{-18}\text{ cm}^{-1}/\text{molecule cm}^{-2}$  at 296 K respectively for the  $\nu_2$  bands of these two isotopes. Partition functions  $Z(296\text{ K}) = 7385$  for  $^{16}\text{O}^{16}\text{O}^{18}\text{O}$  and  $Z(296\text{ K}) = 3599$  for  $^{16}\text{O}^{18}\text{O}^{16}\text{O}$  were used in the calculations.

To check the quality of our calculated parameters, we have compared portions of synthetic spectra with the measured laboratory spectra. The line

parameters from Ref. (5) were included to reproduce absorption features of the  $\nu_2$  and  $2\nu_2-\nu_2$  bands of  $^{16}\text{O}_3$ . As can be seen from Figs. 1 to 3, the agreement between measurement and calculation is very good in all cases.

### CONCLUSIONS

Using high-resolution, room-temperature Fourier transform spectra of  $^{18}\text{O}$ -enriched samples of ozone, we have performed a detailed analysis of the  $\nu_2$  bands of the two monosubstituted isotopic species,  $^{16}\text{O}^{18}\text{O}^{16}\text{O}$  and  $^{16}\text{O}^{16}\text{O}^{18}\text{O}$ . The experimental vibration-rotation energy levels of both molecular species obtained from this analysis combined with the available microwave data were then reproduced to the experimental accuracy with the aid of a Watson A-type Hamiltonian leading to accurate sets of vibrational energies and rotational constants for the ground and the first excited states  $\nu_2$  of the two isotopic species. Because of the difficulties involved in measuring the exact sample purities, the line intensities were computed in the following way. The line intensities of the symmetrical species  $^{16}\text{O}^{18}\text{O}^{16}\text{O}$  were first determined theoretically by transferring the dipole moment of  $^{16}\text{O}_3$ , determined experimentally in earlier studies. Assuming a factor of 2 between the abundances of  $^{16}\text{O}^{16}\text{O}^{18}\text{O}$  and  $^{16}\text{O}^{18}\text{O}^{16}\text{O}$  in the sample produced in the laboratory, experimental intensities were derived for the B-type component of the  $\nu_2$  band of  $^{16}\text{O}^{16}\text{O}^{18}\text{O}$ . The A-type component of the  $\nu_2$  band of  $^{16}\text{O}^{16}\text{O}^{18}\text{O}$  was too weak to be observed in the spectrum. Finally, a list of line positions, intensities, and lower state energies for the  $\nu_2$  band of  $^{16}\text{O}^{18}\text{O}^{16}\text{O}$  and for the B-type component of the  $\nu_2$  band of  $^{16}\text{O}^{16}\text{O}^{18}\text{O}$  was generated providing a complete description of the fine structure of the absorption of the  $^{18}\text{O}$ -monosubstituted ozone isotopes near 14.3  $\mu\text{m}$ .

#### ACKNOWLEDGMENTS

The authors thank Charles T. Solomon of NASA Langley and Rob Hubbard of the National Solar Observatory (NSO) for their help with the Laboratory experiment, Gregg Ladd for the computer processing of the data at NSO, and D. Chris Benner of William and Mary and Carolyn H. Sutton of ST Systems Corporation for their assistance in the processing of the spectra at NASA Langley. Research at the College of William and Mary was supported under Cooperative Agreement NCC1-80 with NASA. The National Solar Observatory is operated by the Association of Universities for Research in Astronomy, Inc., under contract with the National Science Foundation.

## REFERENCES

1. J.-M. Flaud, C. Camy-Peyret, V. Malathy Devi, C. P. Rinsland, and M. A. H. Smith, J. Mol. Spectrosc. 118, 334-344 (1986).
2. C. Camy-Peyret, J.-M. Flaud, A. Perrin, V. Malathy Devi, C. P. Rinsland, and M. A. H. Smith, J. Mol. Spectrosc. 118, 345-354 (1986).
3. J.-M. Flaud, C. Camy-Peyret, V. Malathy Devi, C. P. Rinsland, and M. A. H. Smith, J. Mol. Spectrosc. 122, 221-228 (1987).
4. C. P. Rinsland, V. Malathy Devi, J.-M. Flaud, C. Camy-Peyret, M. A. H. Smith, and G. M. Stokes, J. Geophys. Res. 90, 10719-10725 (1985).
5. H. M. Pickett, E. A. Cohen, L. R. Brown, C. P. Rinsland, M. A. H. Smith, V. Malathy Devi, A. Goldman, A. Barbe, B. Carli, and M. Carlotti, J. Mol. Spectrosc. 128, 151-171 (1988).
6. L. R. Brown and R. A. Toth, J. Opt. Soc. Amer. B 2, 842-856 (1985).
7. C. Chiu and E. A. Cohen, J. Mol. Spectrosc. 109, 239-245 (1985).
8. J.-C. Depannemaecker and J. Bellet, J. Mol. Spectrosc. 66, 106-120 (1977).
9. C. Camy-Peyret and J.-M. Flaud, in "Molecular Spectroscopy: Modern Research" (K. Narahari Rao, Ed.), Vol. III, Academic Press, Orlando, FL, 1985.

## Figure Captions

Figure 1. Spectrum near  $635\text{ cm}^{-1}$  of a room temperature  $^{18}\text{O}$ -enriched ozone sample prepared from an isotopic mixture of oxygen containing  $\sim 85\%$   $^{16}\text{O}_2$  and  $\sim 15\%$   $^{18}\text{O}_2$ . The ozone sample pressure was  $\sim 15.3$  Torr and the absorption path was 50 cm. In this spectral region, the  $P_{Q_{K_a}} = 9$  series of lines belonging to the  $\nu_2$  band of  $^{16}\text{O}^{16}\text{O}^{18}\text{O}$  (solid circles) are observed. The excellent agreement between the observed (solid line) and best-fit calculated (plus symbols) spectra can be noticed.

Figure 2. Laboratory (solid lines) and best-fit calculated (plus symbols) spectra in the region of the  $\nu_2$  band of  $^{16}\text{O}^{18}\text{O}^{16}\text{O}$  around  $732\text{ cm}^{-1}$ . The laboratory spectrum was recorded at room temperature with about 15.3 Torr of ozone in a 50-cm absorption path. The ozone was prepared from an oxygen mixture containing  $\sim 85\%$   $^{16}\text{O}_2$  and  $\sim 15\%$   $^{18}\text{O}_2$ . The  $R_{Q_{K_a}} = 6$  line series (solid circles) is clearly visible and is well reproduced by the calculations.

Figure 3. Laboratory (solid line) and best-fit calculated (plus symbols) spectra in the region of the  $\nu_2$  bands of  $^{16}\text{O}^{18}\text{O}^{16}\text{O}$  and  $^{16}\text{O}^{16}\text{O}^{18}\text{O}$  around  $790.5\text{ cm}^{-1}$ . The laboratory spectrum was recorded at room temperature with about 15.3 Torr of ozone in a 50-cm long absorption cell. The oxygen was generated from an oxygen sample with an initial isotopic composition of  $\sim 85\%$   $^{16}\text{O}_2$  and  $\sim 15\%$   $^{18}\text{O}_2$ . The high J and  $K_a$  transitions of  $^{16}\text{O}^{16}\text{O}^{18}\text{O}$  and  $^{16}\text{O}^{18}\text{O}^{16}\text{O}$  are observed in this spectral region. Their absorptions are well reproduced by the calculations.

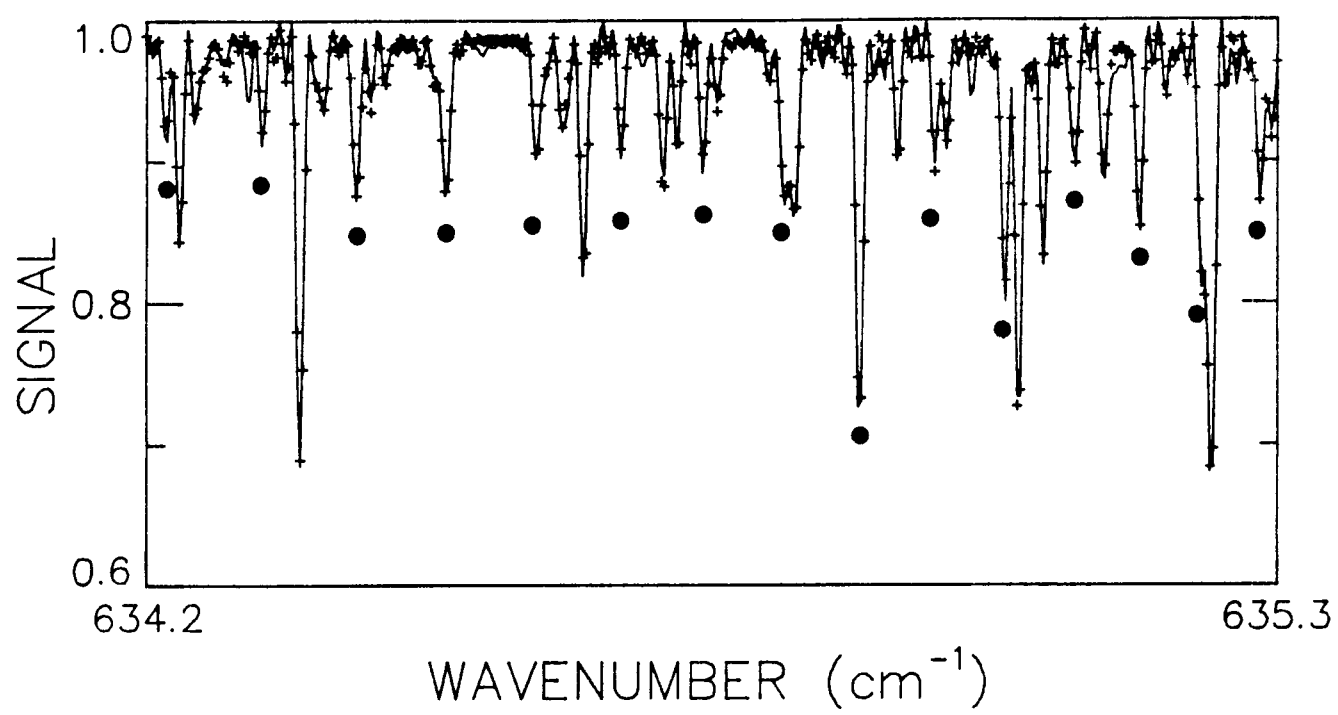
Figure 1

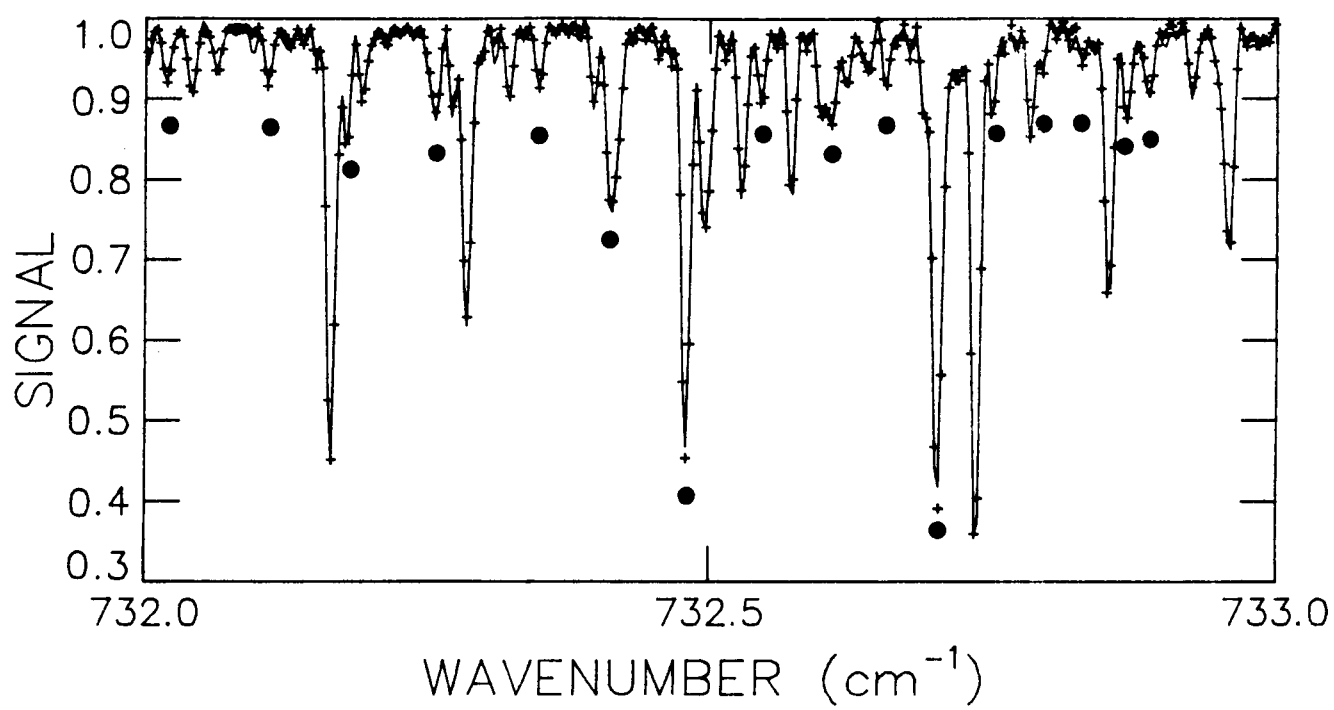
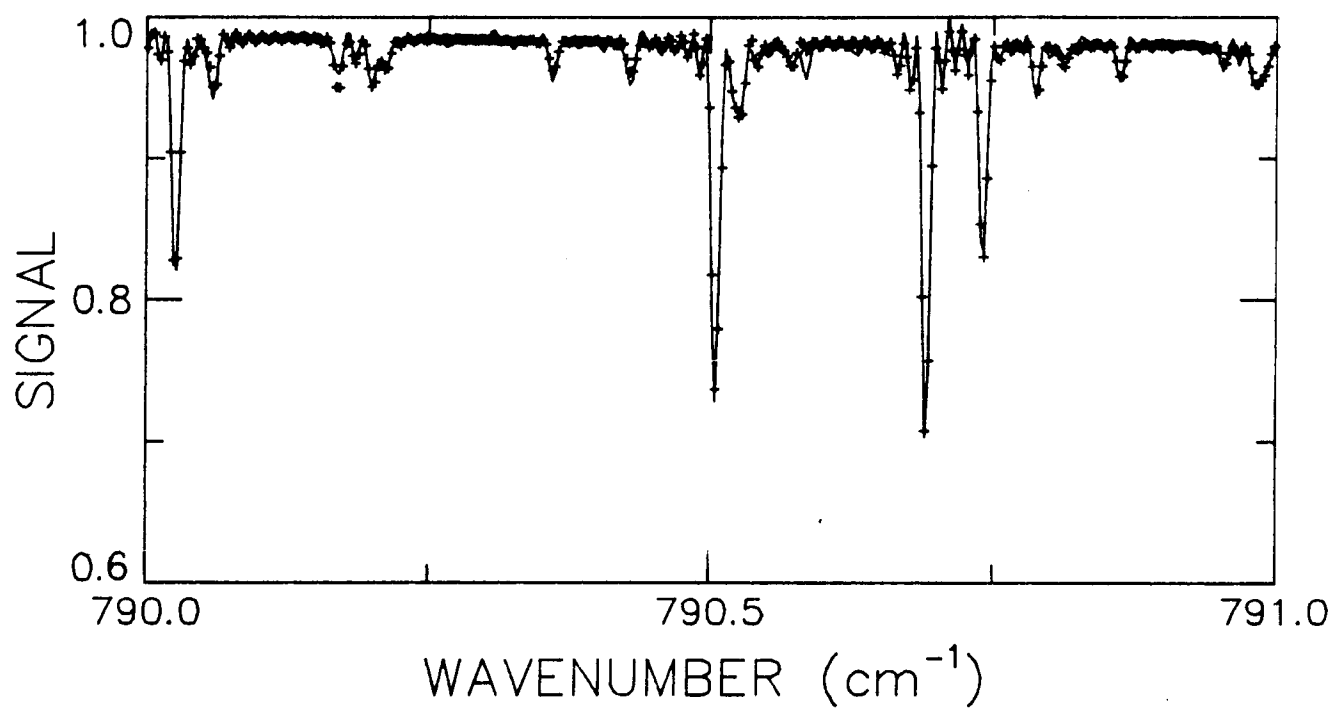
Figure 2

Figure 3

## List of Tables

Table I. Vibrational Energies and Rotational Constants for the (000) and (010) States of  $^{16}\text{O}^{18}\text{O}^{16}\text{O}$ .

Table II. Vibrational Energies and Rotational Constants for the (000) and (010) States of  $^{16}\text{O}^{16}\text{O}^{18}\text{O}$ .

Table III. Transition Moment Operators for the  $\nu_2$  Bands of  $^{16}\text{O}^{18}\text{O}^{16}\text{O}$  and  $^{16}\text{O}^{16}\text{O}^{18}\text{O}$ .

TABLE I  
Vibrational Energies and Rotational Constants for the  
(000) and (010) States of  $^{16}\text{O}^{18}\text{O}^{16}\text{O}$

	(000)	(010)
$E^v$		693.30570 <sub>4</sub> ± 0.000040
$A^v$	3.29049900 <sub>2</sub> ± 0.00000019	3.34155121 <sub>2</sub> ± 0.00000043
$B^v$	0.445399229 <sub>0</sub> ± 0.000000037	0.444188088 <sub>8</sub> ± 0.000000068
$C^v$	0.391329662 <sub>4</sub> ± 0.000000032	0.388900751 <sub>1</sub> ± 0.000000065
$\Delta_K^v$	(0.1808811 <sub>84</sub> ± 0.0000095) × 10 <sup>-3</sup>	(0.1990522 <sub>62</sub> ± 0.0000092) × 10 <sup>-3</sup>
$\Delta_{KJ}^v$	(-0.13179 <sub>52</sub> ± 0.00017) × 10 <sup>-5</sup>	(-0.12424 <sub>81</sub> ± 0.00015) × 10 <sup>-5</sup>
$\Delta_J^v$	(0.44784 <sub>78</sub> ± 0.00011) × 10 <sup>-6</sup>	(0.450826 <sub>77</sub> ± 0.000094) × 10 <sup>-6</sup>
$\delta_K^v$	(0.31155 <sub>99</sub> ± 0.00019) × 10 <sup>-5</sup>	(0.37198 <sub>33</sub> ± 0.00017) × 10 <sup>-5</sup>
$\delta_J^v$	(0.72905 <sub>16</sub> ± 0.00017) × 10 <sup>-7</sup>	(0.72243 <sub>60</sub> ± 0.00011) × 10 <sup>-7</sup>
$H_K^v$	(0.29550 <sub>62</sub> ± 0.00077) × 10 <sup>-7</sup>	(0.37749 <sub>06</sub> ± 0.00064) × 10 <sup>-7</sup>
$H_{KJ}^v$	(-0.1475 <sub>49</sub> ± 0.0022) × 10 <sup>-8</sup>	(-0.1709 <sub>52</sub> ± 0.0012) × 10 <sup>-8</sup>
$H_{JK}^v$	(-0.121 <sub>17</sub> ± 0.050) × 10 <sup>-10</sup>	(-0.25 <sub>63</sub> ± 0.25) × 10 <sup>-11</sup>
$H_J^v$	(0.439 <sub>19</sub> ± 0.083) × 10 <sup>-12</sup>	(0.332 <sub>56</sub> ± 0.046) × 10 <sup>-12</sup>
$h_K^v$	(0.161 <sub>47</sub> ± 0.30) × 10 <sup>-8</sup>	(0.262 <sub>30</sub> ± 0.016) × 10 <sup>-8</sup>
$h_{KJ}^v$	(0.11 <sub>81</sub> ± 0.12) × 10 <sup>-11</sup>	(-0.55 <sub>75</sub> ± 0.32) × 10 <sup>-11</sup>
$h_J^v$	(0.160 <sub>29</sub> ± 0.021) × 10 <sup>-12</sup>	(0.173 <sub>10</sub> ± 0.013) × 10 <sup>-12</sup>
$L_K^v$		(-0.674 <sub>06</sub> ± 0.021) × 10 <sup>-11</sup>

TABLE II

Vibrational Energies and Rotational Constants for the  
(000) and (010) States of  $^{16}\text{O}^{16}\text{O}^{18}\text{O}$

	(000)	(010)
$E^V$		684.61341 <sub>9</sub> ± 0.000027
$A^V$	3.48818507 <sub>8</sub> ± 0.00000013	3.53817681 <sub>6</sub> ± 0.00000030
$B^V$	0.420008328 <sub>1</sub> ± 0.000000022	0.418829269 <sub>3</sub> ± 0.000000038
$C^V$	0.374008935 <sub>3</sub> ± 0.000000020	0.371940160 <sub>1</sub> ± 0.000000036
$\Delta_K^V$	(0.2038845 <sub>76</sub> ± 0.0000064) × 10 <sup>-3</sup>	(0.223517 <sub>86</sub> ± 0.000012) × 10 <sup>-3</sup>
$\Delta_{KJ}^V$	(-0.190229 <sub>10</sub> ± 0.000069) × 10 <sup>-5</sup>	(-0.185794 <sub>93</sub> ± 0.000093) × 10 <sup>-5</sup>
$\Delta_J^V$	(0.406917 <sub>89</sub> ± 0.000040) × 10 <sup>-6</sup>	(0.409396 <sub>49</sub> ± 0.000050) × 10 <sup>-6</sup>
$\delta_K^V$	(0.29205 <sub>51</sub> ± 0.00013) × 10 <sup>-5</sup>	(0.35057 <sub>94</sub> ± 0.00011) × 10 <sup>-5</sup>
$\delta_J^V$	(0.606059 <sub>37</sub> ± 0.000098) × 10 <sup>-7</sup>	(0.602338 <sub>11</sub> ± 0.000063) × 10 <sup>-7</sup>
$H_K^V$	(0.35200 <sub>83</sub> ± 0.00047) × 10 <sup>-7</sup>	(0.44078 <sub>84</sub> ± 0.00078) × 10 <sup>-7</sup>
$H_{KJ}^V$	(-0.1589 <sub>23</sub> ± 0.0014) × 10 <sup>-8</sup>	(-0.1832 <sub>05</sub> ± 0.0013) × 10 <sup>-8</sup>
$H_{JK}^V$	(-0.140 <sub>66</sub> ± 0.029) × 10 <sup>-10</sup>	(-0.92 <sub>34</sub> ± 0.90) × 10 <sup>-12</sup>
$H_J^V$	(0.300 <sub>51</sub> ± 0.024) × 10 <sup>-12</sup>	(0.315 <sub>10</sub> ± 0.023) × 10 <sup>-12</sup>
$h_K^V$	(0.159 <sub>96</sub> ± 0.021) × 10 <sup>-8</sup>	(0.272 <sub>08</sub> ± 0.014) × 10 <sup>-8</sup>
$h_{KJ}^V$	(0.20 <sub>81</sub> ± 0.19) × 10 <sup>-11</sup>	(-0.76 <sub>89</sub> ± 0.20) × 10 <sup>-11</sup>
$h_J^V$	(0.112 <sub>80</sub> ± 0.013) × 10 <sup>-12</sup>	(0.1500 <sub>74</sub> ± 0.0062) × 10 <sup>-12</sup>
$L_K^V$		(-0.523 <sub>83</sub> ± 0.016) × 10 <sup>-11</sup>
$L_{KKJ}^V$		(-0.95 <sub>24</sub> ± 0.67) × 10 <sup>-13</sup>

TABLE III

Transition Moment Operators for the  $\nu_2$  Bands of  
 $^{16}_0^{18}_0^{16}_0$  and  $^{16}_0^{16}_0^{18}_0$

	$^{16}_0^{18}_0^{16}_0$	$^{16}_0^{16}_0^{18}_0$
$\phi_x$	$-0.488 \times 10^{-1}$	$(-0.49500_3 \pm 0.00035) \times 10^{-1}$
$\{i\phi_y, J_z\}$	$0.194 \times 10^{-3}$	$(0.2772_6 \pm 0.0021) \times 10^{-3}$
$\{\phi_z, iJ_y\}$	$0.135 \times 10^{-3}$	$(0.1475_1 \pm 0.0011) \times 10^{-3}$

All the results are in Debye and the quoted errors correspond to one standard deviation.

As explained in the text, only the B-type component of the  $\nu_2$  band of  $^{16}_0^{16}_0^{18}_0$  was observed.

## List of Symbols

$\nu$  = lower case Greek letter nu

$\Delta$  = upper case Greek letter delta

$\delta$  = lower case Greek letter delta

$\phi$  = lower case Greek letter phi